AMERICAN SOCIETY FOR MICROBIOLOGY | Applied and Environmental Microbiology®

ENZYMOLOGY AND PROTEIN ENGINEERING

Enzyme Activities of Two Recombinant Heme-Containing Peroxidases, *Tv*DyP1 and *Tv*VP2, Identified from the Secretome of *Trametes versicolor*

Sawsan Amara,[a] Thomas Perrot,[b] David Navarro,[a,c] Aurélie Deroy,[b] Amine Benkhelfallah,[a] Amani Chalak,[a] Marianne Daou,[a] Didier Chevret,[d] Craig B. Faulds,[a] Jean-Guy Berrin,[a] Mélanie Morel-Rouhier,[b] Eric Gelhaye,[b] Eric Record[a]

[a]INRA, Aix-Marseille Université, UMR1163, Biodiversité et Biotechnologie Fongiques, Marseille, France
[b]INRA, UMR 1136, Interactions Arbres/Micro-Organismes, Champenoux, France
[c]Centre International de Ressources Microbiennes-Champignons Filamenteux, UMR1163 BBF, Marseille, France
[d]PAPPSO, Micalis Institute, INRA, AgroParisTech, Université Paris-Saclay, Jouy-en-Josas, France

ABSTRACT *Trametes versicolor* is a wood-inhabiting agaricomycete known for its ability to cause strong white-rot decay on hardwood and for its high tolerance of phenolic compounds. The goal of the present work was to gain insights into the molecular biology and biochemistry of the heme-including class II and dye-decolorizing peroxidases secreted by this fungus. Proteomic analysis of the secretome of *T. versicolor* BRFM 1218 grown on oak wood revealed a set of 200 secreted proteins, among which were the dye-decolorizing peroxidase *Tv*DyP1 and the versatile peroxidase *Tv*VP2. Both peroxidases were heterologously produced in *Escherichia coli*, biochemically characterized, and tested for the ability to oxidize complex substrates. Both peroxidases were found to be active against several substrates under acidic conditions, and *Tv*DyP1 was very stable over a relatively large pH range of 2.0 to 6.0, while *Tv*VP2 was more stable at pH 5.0 to 6.0 only. The thermostability of both enzymes was also tested, and *Tv*DyP1 was globally found to be more stable than *Tv*VP2. After 180 min of incubation at temperatures ranging from 30 to 50°C, the activity of *Tv*VP2 drastically decreased, with 10 to 30% of the initial activity retained. Under the same conditions, *Tv*DyP1 retained 20 to 80% of its enzyme activity. The two proteins were catalytically characterized, and *Tv*VP2 was shown to accept a wider range of reducing substrates than *Tv*DyP1. Furthermore, both enzymes were found to be active against two flavonoids, quercetin and catechin, found in oak wood, with *Tv*VP2 displaying more rapid oxidation of the two compounds. They were tested for the ability to decolorize five industrial dyes, and *Tv*VP2 presented a greater ability to oxidize and decolorize the dye substrates than *Tv*DyP1.

IMPORTANCE *Trametes versicolor* is a wood-inhabiting agaricomycete known for its ability to cause strong white-rot decay on hardwood and for its high tolerance of phenolic compounds. Among white-rot fungi, the basidiomycete *T. versicolor* has been extensively studied for its ability to degrade wood, specifically lignin, thanks to an extracellular oxidative enzymatic system. The corresponding oxidative system was previously studied in several works for classical lignin and manganese peroxidases, and in this study, two new components of the oxidative system of *T. versicolor*, one dye-decolorizing peroxidase and one versatile peroxidase, were biochemically characterized in depth and compared to other fungal peroxidases.

KEYWORDS *Trametes versicolor*, white-rot fungus, dye-decolorizing peroxidase, versatile peroxidase, class II heme peroxidase, fungal secretome

Received 20 December 2017 **Accepted** 4 February 2018

Accepted manuscript posted online 16 February 2018

Citation Amara S, Perrot T, Navarro D, Deroy A, Benkhelfallah A, Chalak A, Daou M, Chevret D, Faulds CB, Berrin J-G, Morel-Rouhier M, Gelhaye E, Record E. 2018. Enzyme activities of two recombinant heme-containing peroxidases, *Tv*DyP1 and *Tv*VP2, identified from the secretome of *Trametes versicolor*. Appl Environ Microbiol 84:e02826-17. https://doi.org/10.1128/AEM.02826-17.

Editor Robert M. Kelly, North Carolina State University

Address correspondence to Sawsan Amara, sawsan.amara81@gmail.com, or Eric Record, eric.record@inra.fr.

Basidiomycetous white-rot fungi are unique in the ability to degrade all polymeric components of wood and other lignocellulosic substrates. Interest in this group of fungi and their lignocellulolytic system has increased because of their biotechnological potential for the biodegradation of various recalcitrant and environmental pollutants, including toxic chemicals (1). Thanks to the recent release of more than 60 Basidiomycota genomes (2, 3), extensions of gene families encoding plant cell wall-degrading enzymes have been proposed to be characteristic of wood-decaying Agaricomycetes species (2). Among white-rot fungi, the basidiomycete *Trametes versicolor* has often been studied as an efficient degrader of wood and possesses a nonspecific extracellular oxidative enzymatic system capable of degrading complex polymeric and phenolic materials (4–8). The *T. versicolor* genome was sequenced and revealed a large number of class II peroxidases and laccases, with 26 and 10 putative representatives, respectively (3, 9). The laccases (EC 1.10.3.2) are among the most common extracellular oxidoreductases secreted by *T. versicolor* (10). In addition, various heme-including peroxidases, mainly manganese peroxidases (MnPs, EC 1.11.1.13) and lignin peroxidases (LiPs, EC 1.11.1.14), have been reported to be secreted by this fungus (11, 12). A third type of lignin-modifying peroxidase named versatile peroxidase (VP, EC 1.11.1.16) has been described in fungi of the genera *Pleurotus* and *Bjerkandera* (13–15). VP is a lignin-modifying peroxidase that has some of the catalytic properties of MnP and LiP (16, 17) and is thus capable of oxidizing the typical substrates of both MnP (Mn^{2+}) and LiP (veratryl alcohol [VA]).

Recently, the secretome of *T. versicolor* BAFC 2234 grown on tomato juice medium supplemented with copper and manganese was analyzed and the secreted lignin-modifying enzymes (a laccase, three MnP isoforms, and one VP isoform) were partially purified (18). However, no biochemical characterization of the purified peroxidases was carried out.

The heme-including peroxidases were traditionally classified on the basis of their sequence similarities and structural properties into classes I (prokaryotic and eukaryotic organelle), II (fungus secreted), and III (plant secreted) (19). This classification included most of the known heme peroxidases until the discovery of new heme-including peroxidase types in the last decades. This resulted in two novel superfamilies of fungus-secreted heme-including peroxidases: heme-thiolate peroxidases (HTPs, UPOs) (20) and dye-decolorizing peroxidases (DyPs) (20, 21). DyPs constitute a divergent protein superfamily distantly related to the catalase-peroxidase superfamily comprising the class I, II, and III peroxidases (20).

A high number of putative DyP sequences are available in protein databases (233 DyP sequences from fungal, bacterial, and archaeal genomes [http://peroxibase.toulouse.inra.fr]), and fungal DyPs from *Bjerkandera adusta* (22), *Termitomyces albuminosus* (23), *Marasmius scorodonius* (24), *Auricularia auricula-judae* (25), *Irpex lacteus* (26), *Exidia glandulosa*, and *Mycena epipterygia* (27) have been purified and enzymatically characterized. Some DyPs present interesting characteristics such as resistance to high temperatures (28, 29) and pressures (24) and stability under acidic conditions (25, 28, 29). Moreover, the catalytic mechanisms of a number of representatives have been described and their protein structures have been elucidated (27, 30–32).

In this work, we studied two peroxidases identified in the secretome of *T. versicolor* BRFM 1218 grown on wood-containing medium. These two enzymes were characterized in regard to their capacity to oxidize complex substrates and tested for the capacity to decolorize industrial dyes.

RESULTS

Peroxidase selection. The secretome of *T. versicolor* BRFM 1218 grown on malt agar wood was analyzed by using proteomics (Table 1). Among the 200 proteins identified in the secretomes, 21 peroxidases were identified in the secretome and are listed in the order of relative abundance in Table 1. *Tv*DyP1 and *Tv*VP2 were selected to study the oxidative system of *T. versicolor* because (i) they represent new peroxidase models, as LiPs and MnPs from *T. versicolor* were extensively studied in previous works; (ii) they are

TABLE 1 Abundance of peroxidase enzymes in secretomes during growth on malt agar wood[a]

JGI Prot Id (genome of *Trametes versicolor*)	Functional annotation	Protein abundance index (PAI)
jgi|Trave1|43578	LiP2	5.40
jgi|Trave1|112835	MnP2	3.14
jgi|Trave1|114944	LiP12	2.67
jgi|Trave1|133731	LiP8	2.67
jgi|Trave1|43477	MnP5s	2.42
jgi|Trave1|52333	LiP6	2.33
jgi|Trave1|48870	**DyP1 Dyp-type peroxidase**	1.85
jgi|Trave1|130496	MnP4	1.27
jgi|Trave1|131080	MnP3	1.27
jgi|Trave1|133918	LiP3	1.14
jgi|Trave1|51455	MnP6	1.00
jgi|Trave1|51457	MnP9	0.92
jgi|Trave1|133326	LiP4	0.89
jgi|Trave1|26239	**VP2**	0.75
jgi|Trave1|51442	MnP13	0.63
jgi|Trave1|134657	LiP10	0.57
jgi|Trave1|134226	LiP9	0.50
jgi|Trave1|51375	MnP1	0.43
jgi|Trave1|48874	Dyp-type peroxidase	0.29
jgi|Trave1|43576	LiP1	0.22
jgi|Trave1|51451	MnP7	0.22
jgi|Trave1|44897	MnP10	nd
jgi|Trave1|74595	MnP11s	nd
jgi|Trave1|43289	VP1	nd
jgi|Trave1|74179	MnP8s	nd
jgi|Trave1|28895	VP3at	nd

[a]Peptide abundance is indicated by green and yellow shading. Protein models were taken from the JGI MycoCosm *T. versicolor* genome site. nd, not detected. Enzymes selected for the present study are in red.

cosecreted with other class II peroxidases, which suggests a physiological function important to the fungus; and (iii) of the DyP and VP representatives identified in the secretome, they were by far the most abundant.

Enzyme production and purification. (i) Production of *Tv*DyP1 in a soluble and active form. For heterologous expression of *Tv*DyP1, a 5-liter culture of *Escherichia coli* transformants was prepared, resulting in production of *Tv*DyP1 as an active protein. After a lysis step, the enzyme was purified in two different chromatographic steps. As shown by sodium dodecyl sulfate-polyacrylamide gel electrophoresis (SDS-PAGE) monitoring of the purification process (Fig. 1A), the soluble fraction (lane 1) from the *E. coli*

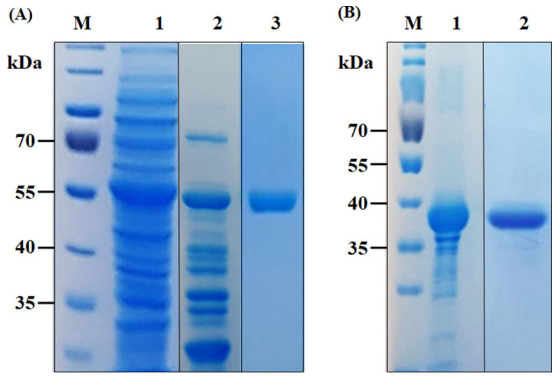

FIG 1 SDS-PAGE illustrating the production and different purification steps for *T. versicolor* peroxidases produced in *E. coli*. (A) Two-step purification of *Tv*DyP1. Lanes: 1, *E. coli* soluble fraction containing *Tv*DyP1; 2, first purification step on a Mono Q column; 3, pure DyP obtained after Q-Sepharose chromatography; M, protein molecular mass markers. (B) One-step purification of *Tv*VP2. Lanes: 1, renatured inclusion bodies; 2, pure *Tv*VP2 obtained after Mono Q column chromatography; M, protein molecular mass markers. In panels A and B, the different lanes are from different gels that were run for the same period of time.

TABLE 2 N-terminal sequences and molecular masses of *Tv*DyP1 and *Tv*VP2 from *T. versicolor* produced in *E. coli*

Characteristic	*Tv*DyP1	*Tv*VP2
Molecular mass (kDa)		
Theoretical	52.17	36.25
Determined	52.036, 52.714	36.375
N-terminal sequence		
Theoretical	MSSTVP	MVPSA
Determined	SSTVP	MVPSA

cultures was considerably enriched in the *Tv*DyP1 (52 kDa) band after the first Mono Q chromatography step. However, several other proteins were still present.

These contaminating proteins were removed by the second Q-Sepharose chromatography step. Homogeneous *Tv*DyP1 was obtained (lane 3) with a purification yield of 5 mg of protein/5-liter *E. coli* culture and a Reinheitzahl (Rz) A_{405}/A_{280} ratio of ~2.

(ii) Production of *Tv*VP2 as inclusion bodies and *in vitro* folding and activation. For heterologous expression of *Tv*VP2, a 5-liter culture of *E. coli* transformants was grown and after lysis, a large quantity of protein (about 120 mg · liter^{-1}) was found accumulated in insoluble inclusion bodies (Fig. 1B, lane 1). *In vitro* activation of *E. coli*-expressed *Tv*VP2 was carried out under conditions previously optimized for other peroxidases (33), i.e., folding in 50 mM Tris-HCl (pH 9.5) containing 20 μM hemin, 0.16 M urea, 5 mM Ca^{2+}, 0.5 mM oxidized glutathione, 0.1 mM dithiothreitol (DTT), and 0.1 mg · ml^{-1} protein for ~20 h at room temperature. The mixture was then concentrated, dialyzed, and centrifuged, allowing the elimination of folding additives and unfolded protein. *Tv*VP2 was purified by a single anion-exchange chromatographic step with a Mono Q column (see Fig. S1B in the supplemental material). SDS-PAGE analysis of purified *Tv*VP2 shows a single band of protein (lane 2) with a molecular mass of ~37 kDa. A purification yield of 30 mg of purified and active protein/5-liter *E. coli* culture with an Rz A_{405}/A_{280} ratio of ~3 was obtained.

N-terminal sequence and MS analyses. The N-terminal amino acid sequences were analyzed by sequential Edman degradation and confirmed the first five residues predicted from the protein sequence (Table 2), except for the first amino acid (methionine) of *Tv*DyP1, which was missing. Mass spectrometry (MS) analysis (Table 2) showed two major peaks of *Tv*DyP1 at 52.036 and 52.714 kDa, in agreement with the molecular mass calculated from the amino acid sequence (52,171 Da). A minor peak (~10%) was recorded at 49,118 Da, which might correspond to the partial degradation of *Tv*DyP1 during the purification procedure, although a protease inhibitor was added to the lysis buffer. Mass spectrometric analysis of *Tv*VP2 (Table 2) showed a major peak corresponding a molecular mass of 36,375 Da, which is slightly lower than that of wild-type *Tv*VP2 purified from fungal cultures (44.6 kDa) (18), probably because of the lack of glycosylation machinery in *E. coli*, but in agreement with that calculated from the amino acid sequence (36.25 kDa).

Enzyme characterization. (i) Temperature stability of *Tv*DyP1 and *Tv*VP2. The thermostability of *Tv*DyP1 and *Tv*VP2 was examined by measuring the oxidation of 2,2′-azinobis(3-ethylbenzthiazolinesulfonic acid) (ABTS) after heat treatment of the enzymes at different temperatures. Both were found to be sensitive to high temperatures (60 to 70°C), with >80% of their activity lost after 30 min of incubation at 60°C, while no activity was measured for the same incubation time at 70°C (Fig. 2A and B). Similar patterns were observed with both enzymes at temperatures ranging from 30 to 50°C after 30 min of incubation, with 100 and 80% residual activity of *Tv*DyP1 (Fig. 2A) and *Tv*VP2 (Fig. 2B) measured, respectively. Beyond 30 min of incubation, activity decreased drastically, with the greater effect on *Tv*VP2 with only 10 to 30% residual activity measured after 180 min of incubation at temperatures ranging from 30 to 50°C (Fig. 2B). Under the same conditions, *Tv*DyP1 retained 20 to 80% of its initial activity (Fig. 2A). The thermal inactivation profiles of both enzymes (data not shown) showed

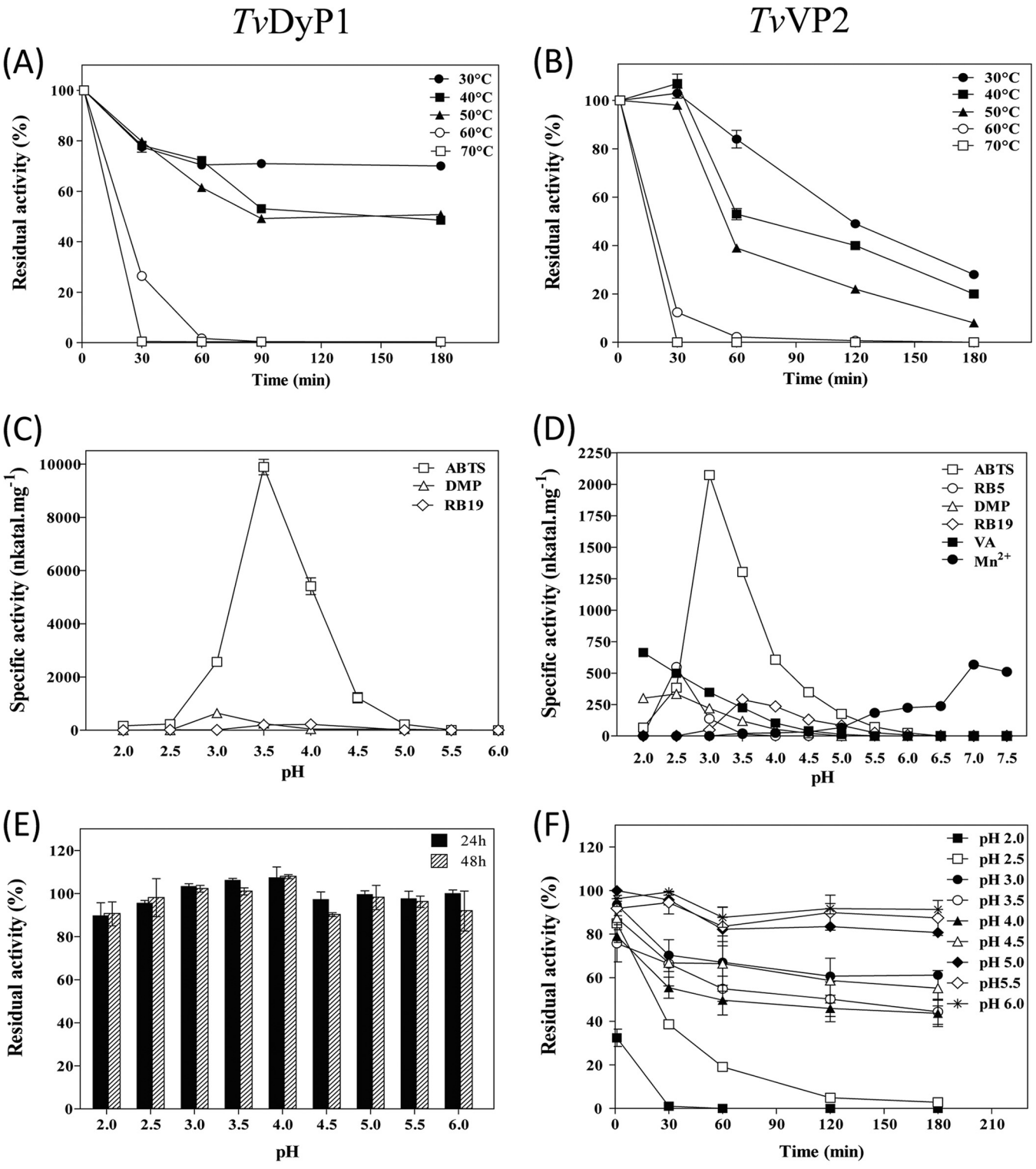

FIG 2 Physicochemical characterization of recombinant enzymes. The thermal stability of *Tv*DyP1 (A) and *Tv*VP2 (B) from *T. versicolor* produced in *E. coli* was determined. Residual activities were estimated after 30, 60, 120, and 180 min of incubation at temperatures ranging from 30 to 70°C and referred to the activity measured immediately after addition of the enzyme. The optimal pHs for the oxidation of ABTS (5 mM), DMP (20 mM), RB5 (30 μM), RB19 (200 μM), VA (20 mM), and Mn^{2+} (10 mM) in 0.1 M tartrate buffer by *Tv*DyP1 (C) and *Tv*VP2 (D) from *T. versicolor* produced in *E. coli* were determined. The pH stability of *Tv*DyP1 (E) and *Tv*VP2 (F) from *T. versicolor* produced in *E. coli* was determined. Residual activities were calculated after 24 or 48 h of incubation for *Tv*DyP1 or after 30, 60, 120, and 180 min for *Tv*VP2 at pH 2 to 6 in 0.1 M tartrate and referred to the activity measured immediately after addition of the enzyme. Each data point (mean ± standard deviation) is the result of triplicate experiments.

that they were rather stable, with half-inactivation temperatures (60 min) of 51.7 and 52.2°C estimated for *Tv*DyP1 and *Tv*VP2, respectively.

(ii) Effect of pH on *Tv*DyP1 and *Tv*VP2 activity and stability. The effect of pH on *Tv*DyP1 and *Tv*VP2 activities was initially examined with different substrates at pHs ranging from 2.0 to 7.5. As shown in Fig. 2C and D, both peroxidases were active at acidic pHs ranging from 2.0 to 5.0, although there were some exceptions; i.e., no *Tv*DyP1 activity was recorded on VA, Reactive Black 5 (RB5), or Mn^{2+} at any pH tested (Fig. 2C), while maximum *Tv*VP2 activity on Mn^{2+} was obtained at pH 7.0 (Fig. 2D). On the other hand, the specific activities and optimum pHs of both enzymes differed depending on the substrates tested. *Tv*VP2 presents a broader substrate specificity than *Tv*DyP1, and both enzymes were more active on ABTS than on any other substrate (9,892 and 2,074 nkat · mg^{-1} for *Tv*DyP1 and *Tv*VP2, respectively). Oxidation of this substrate occurred at similar pHs with both enzymes (3.5 and 3.0 for *Tv*DyP1 and *Tv*VP2, respectively), and activities decreased drastically at pHs beyond 4.5.

Similar pH profiles of *Tv*VP2 oxidation of VA and 2,6-dimethoxyphenol (DMP) were obtained, with an optimal pH of 2 to 2.5 and a 40% reduction of activity at pH 3.0. The optimum pH for RB5 oxidation was also pH 2.5, but in this case, the enzyme lost ~75% of its activity at pH 3.0. DMP oxidation by *Tv*DyP1 was, however, obtained at an optimal pH of 3.0. Reactive Blue 19 (RB19) decolorization by *Tv*VP2 was optimal at pH 3.5. In contrast, the highest optimal pH of 7.0 was observed for Mn^{2+} oxidation.

The pH stability of *Tv*DyP1 was studied by incubating the enzyme at pHs 2 to 6 at 4°C. As the protein was very stable in relation to pH, only results for 24 and 48 h of incubation are shown (Fig. 2E). The enzyme was found to be very stable at all of the pHs studied, since it retained ~90% of its initial activity even after 48 h of incubation. For *Tv*VP2 stability, shorter incubation times (30, 60, 120, and 180 min) were tested since the enzyme was more sensitive to pH (Fig. 2F). At acidic pHs (2 to 2.5), the enzyme was totally inactivated after the first 30 min of incubation at pH 2.0 and after 2 h of incubation at pH 2.5. At pHs ranging from 3.0 to 4.5, *Tv*VP2 retained 50 to 70% of its initial activity after 3 h of incubation at 4°C. A more stable profile pattern of *Tv*VP2 was observed at pHs 5.0 to 6.0, with >80% residual activity remaining after 3 h of incubation.

(iii) Catalytic properties. *Tv*DyP1 and *Tv*VP2 were tested on six representative substrates, and the kinetic constants obtained are shown in Table 3. Significant differences between the two peroxidases were observed. Of the six substrates tested, *Tv*DyP1 exhibited an affinity for only three, ABTS, DMP, and RB19 (K_m, 37.8 to 292.6 μM), while no activity was detected on RB5, VA, or Mn^{2+}. As observed for other fungal DyPs, the highest turnover value of *Tv*DyP1 from *T. versicolor* was found for ABTS (k_{cat}, 581.1 s^{-1}), followed by DMP (k_{cat}, 87.4 s^{-1}) and the anthraquinone dye RB19 (k_{cat}, 23.8 s^{-1}) (28). *Tv*VP2 was found to possess an affinity for the six substrates, with the highest for RB5 and RB19. The oxidation of the low-redox-potential dye ABTS by *Tv*VP2 was found to be lower (k_{cat}, 79.2 s^{-1}) than that by *Tv*DyP1 (Table 3). Moreover, *Tv*DyP1 presented a slightly higher apparent affinity for ABTS than *Tv*VP2 (K_m, 292.2 and 415 μM, respectively), with an even better k_{cat} (582 and 79.2 s^{-1}, respectively); consequently, *Tv*DyP1 was ~10-fold more efficient than *Tv*VP2 on this substrate (k_{cat}/K_m, 1,989.4 and 190.8 s^{-1} mM^{-1}, respectively).

(iv) Effect of H_2O_2. Peroxidases tend to lose activity in the presence of H_2O_2 through a mechanism-based process known as suicide inactivation (34). The optimum H_2O_2 concentration for *Tv*DyP1 and *Tv*VP2 depended on the substrate used (Fig. 3). Optimal H_2O_2 concentrations of 0.25 and 0.5 mM were obtained with ABTS as a substrate for *Tv*VP2 and *Tv*DyP1, respectively. Then the activity decreased gradually to <30% residual activity fof both enzymes at 5.0 mM H_2O_2. Interestingly, *Tv*VP2 displayed significant activity in the absence of H_2O_2 at 7.5% of its maximal activity.

(v) Oxidation of flavonoids by peroxidases. The capacity of both peroxidases to oxidize catechin (CAT) and quercetin (QUE), which are extractable from oak wood (35), was investigated. *Tv*VP2, in the presence of hydrogen peroxide (0.1 mM), altered the

TABLE 3 Kinetic constants[a] of oxidation of different aromatic and nonaromatic dyes by *Tv*DyP1 and *Tv*VP2 from *T. versicolor* produced in *E. coli*

Substrate and parameter	*Tv*DyP1	*Tv*VP2
ABTS		
K_m	292.6 ± 50.24	415 ± 42
k_{cat}	582.1 ± 0.05	79.2 ± 2
k_{cat}/K_m	1,989.4	190.8
pH	3.5	3.0
RB5		
K_m	0	10.2 ± 0.9
k_{cat}	0	26.8 ± 0.86
k_{cat}/K_m	0	2,640
pH	2.0–5.0	2.5
DMP		
K_m	1,026 ± 78.52	2,597 ± 196
k_{cat}	87.4 ± 0.08	13.8 ± 0.24
k_{cat}/K_m	85.2	5.3
pH	3.0	2.5
RB19		
K_m	37.8 ± 3.34	31.2 ± 3.13
k_{cat}	23.8 ± 0.62	19.2 ± 0.63
k_{cat}/K_m	629.6	615.4
pH	4.0	3.5
VA		
K_m	0	9,995 ± 1,279
k_{cat}	0	31.2 ± 1.5
k_{cat}/K_m	0	3.1
pH	2.0–5.0	2.0
Mn^{2+}		
K_m	0	958.5 ± 66
k_{cat}	0	22.6 ± 0.33
k_{cat}/K_m	0	23.6
pH	4.0–7.0	7.0

[a] K_m, μM; k_{cat}, s^{-1}; k_{cat}/K_m, s^{-1} mM^{-1}.

250- to 600-nm absorbance spectra of CAT recorded every 60 s over a 4-min period, while the modification of absorbance by *Tv*DyP1 was weaker in the 400-nm region of the spectrum (Fig. 4A and B; Fig. S1 and S2A and B). A major increase in optical density at around 400 nm was observed, suggesting the formation of quinones (36). The same approach was used with QUE (Fig. S3). In this case, incubation of the flavonoid with both peroxidases in the presence of hydrogen peroxide led to strong modification of the observed spectra, in particular, a decrease of the 370 nm peak (Fig. 4C and D; Fig. S4A and B). As observed for CAT (Fig. S2C and D), the observed modification induced by *Tv*VP2 seemed to be greater than that induced by *Tv*DyP1 (Fig. S4C and D). Interestingly, the UV spectrum of QUE oxidation by *Tv*VP2 showed a small increase in absorption at around 290 nm, which was not detected after oxidation by *Tv*DyP1. This absorption band could match the production of 3,4-dihydroxybenzoic acid (37). Using reverse chromatography to analyze the reactional mixtures, we noticed that the CAT signal was dramatically decreased or lost after oxidation by *Tv*DyP1 and *Tv*VP2, respectively (data not shown). Nevertheless, no additional peaks were observed in chromatograms, suggesting that the quinones polymerized, and their detection was not possible by this method. The production of insoluble brown compounds was indeed observed, preventing any further characterization by chromatographic steps.

(vi) Decolorization of industrial dyes. To study the abilities of *Tv*DyP1 and *Tv*VP2 to oxidize complex substrates, five industrial dyes were selected from different usages and chemical structures (acidic, basic, reactive, vat, and disperse dyes). As shown in

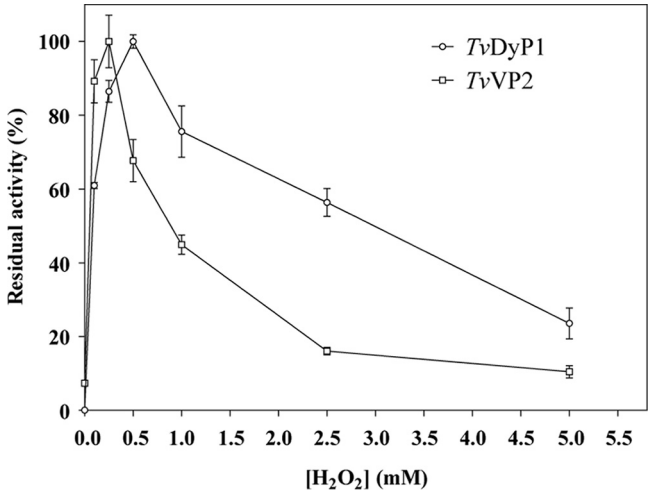

FIG 3 Effect of H_2O_2 on the activities of recombinant *Tv*DyP1 and *Tv*VP2. Activities were determined under standard assay conditions at the optimal pH for each enzyme (3.0 for *Tv*VP2 and 3.5 for *Tv*DyP1) in the presence of H_2O_2 (0 to 5 mM). Each data point (mean ± standard deviation) is the result of triplicate experiments.

Table 4, both peroxidases were active on Acid Black 172 (AB) dye, with a slightly higher decolorization percentage for *Tv*VP2 than for *Tv*DyP1. Regarding the other dyes, *Tv*VP2 presented a wider range of action since it was also active on Basic Blue 41 (BB) and Reactive Black (RB).

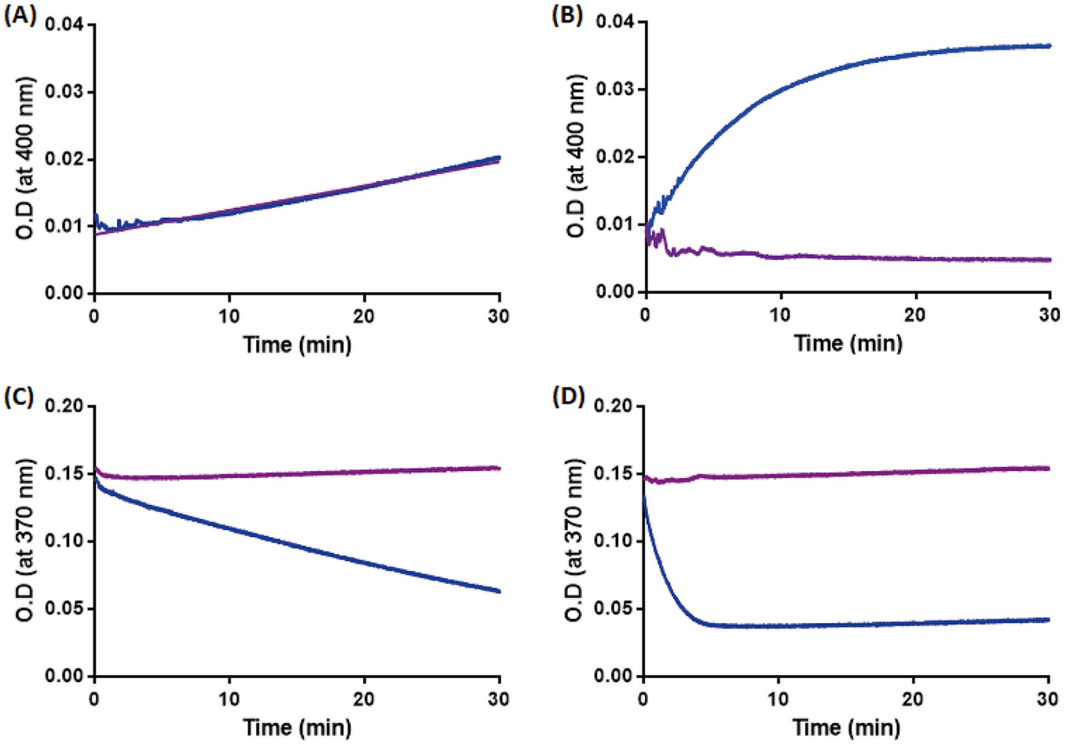

FIG 4 Changes in absorbance over 30 min during the oxidation of CAT (10 μM) and QUE (10 μM) by peroxidases. (A) Oxidation of CAT (10 μM) by *Tv*DyP1 alone (0.2 μM), purple; oxidation of CAT (10 μM) by *Tv*DyP1 (0.2 μM) with H_2O_2 (1 mM), blue. (B) Oxidation of CAT (10 μM) by *Tv*VP2 alone (0.2 μM), purple; oxidation of CAT (10 μM) by *Tv*VP2 (0.2 μM) with H_2O_2 (1 mM), blue. The curve for CAT oxidized by *Tv*DyP1 alone has been rearranged to begin at the same point as the other curves. (C) Oxidation of QUE (10 μM) by *Tv*DyP1 alone (0.2 μM), purple; oxidation of QUE (10 μM) by *Tv*DyP1 (0.2 μM) with H_2O_2 (1 mM), blue. (D) Oxidation of QUE (10 μM) by *Tv*VP2 alone (0.2 μM), purple; oxidation of QUE (10 μM) by *Tv*VP2 (0.2 μM) with H_2O_2 (1 mM), blue. O.D., optical density.

TABLE 4 Decolorization of industrial dyes by *Tv*DyP1 and *Tv*VP2[a]

Dye	*Tv*DyP1	*Tv*VP2
AB	++	++
BB	−	+
RB5	−	+
DB	−	−
VG	−	−

[a]Decolorization was determined after 1 h of incubation at pHs 2.5, 3, and 3.5 at 37°C. Symbols: −, no decolorization; +, 30% of minimum decolorization; ++, 75% of minimum decolorization.

DISCUSSION

In the present study, *T. versicolor* was selected among diverse wood-inhabiting Agaricomycetes because of its ability to cause a strong white rot on hardwood and the strain BRFM 1218 was cultivated in the presence of oak sapwood. Several peroxidases were identified by proteomic analysis, and two peroxidases, *Tv*DyP1 and *Tv*VP2, were selected for functional characterization, including biochemical characterization, and testing for decolorization of industrial dyes. In this context, we report the production and purification of *Tv*DyP1 from *T. versicolor*. We used a previously described approach consisting of DyP production in a soluble and active form (28). Similar protein production yields were reached with the two *Pleurotus ostreatus* DyP isoforms *Po*DyP1 and *Po*DyP4 (6.3 and 11.7 mg/9 liters of *E. coli* culture, respectively). *Po*DyP4, sharing 52% amino acid sequence identity with *T. versicolor Tv*DyP1, presents the highest-identity sequence. DyP from *Bjerkandera adusta*, incorrectly named *Thanatephorus cucumeris* (38), was the first DyP heterologously expressed as an active and soluble enzyme in both *Aspergillus oryzae* (39) and *E. coli* (40) after laborious purification steps, giving a limited biochemical characterization of two isoforms, named DyP2 and DyP3 (41).

To produce *Tv*VP2 from *T. versicolor*, we used the same expression protocol as for *Tv*DyP1. However, attempts to get the *Tv*VP2 peroxidase as a soluble and active enzyme failed even after optimization assays (data not shown). Therefore, the protein was first produced as inclusion bodies and then the enzyme was recovered and activated *in vitro* in accordance with the previously optimized protocol for other VPs (28, 33, 42). Although native *Tv*VP2 was previously purified from the secretome of *T. versicolor* grown on tomato juice medium, a very low yield of protein was obtained and no biochemical characterization was performed (18).

In agreement with their different phylogenetic origins, *T. versicolor Tv*DyP1 and *Tv*VP2 differed significantly in kinetics and stability. Compared to other DyPs, *T. versicolor Tv*DyP1, together with *B. adusta* native DyP (40) and *Po*DyP4, was more thermostable than the previously described fungal DyPs, as well as *Tv*VP2. *Tv*DyP1 was, however, less thermostable than *B. adusta* DyP, which retains 92% of its initial activity after incubation at 60°C for 60 min (40).

*Tv*DyP1 was found to be stable over a large range of pHs, with an optimal activity at acidic pH. This stability pattern was similar to that observed in other fungal DyPs, being >80% stable after 24 h at pH 2 (28, 29). However, *Tv*VP2 was more sensitive to acidic pH and was more stable at pH 5 to 6. In comparison, VP from *Pleurotus eryngii* has similar behavior concerning this parameter (43), and this relatively low observed pH stability of fungal peroxidases is a drawback in their industrial application (33). Therefore, the pH stability of *Po*VP was improved by direct mutagenesis (43).

The pH optima of *Tv*DyP1 and *Tv*VP2 were found to be similar to those previously described for *Po*DyP1 and *Po*DyP4, with an optimum at pH 3 to 4 for the phenolic and dye substrates and a higher optimum pH of 4.5 for Mn^{2+}, suggesting the involvement of deprotonated acidic residues in the latter activity (28). Related to the substrate specificity of fungal class II peroxidases such as DyPs and VPs, acidic conditions are required for the optimum oxidative activity of the enzyme, with an even more acidic optimum pH of <3 in the case of nonphenolic aromatic substrates such as VA. In the same way, the optimum pH for VA oxidation by *Tv*VP2 was found to be 2, while *Tv*DyP1 was unable to oxidize this substrate. This substrate is either not (29) or poorly (26)

oxidized by other fungal DyPs. A similar pattern was previously reported for *B. adusta* DyP, with an acidic optimum pH of 3.2 obtained with all of the substrates tested, as well as an absence of activity on VA (41, 43).

The specificity of the two recombinant enzymes was discriminated on five substrates, including dyes, aromatics, and nonaromatics (Table 4). Under our conditions, *Tv*VP2 was demonstrated to be more versatile than *Tv*DyP1. Considering the kinetic properties, *Tv*VP2 displayed a low affinity for VA (K_m, 9,995 μM). This low affinity was similar to that reported for *Po*VP isoenzyme 2 (33) but lower than those reported for well-characterized lignin-modifying class II peroxidases, being ~2- to 6-fold lower than that of *Po*VP isoenzymes 1 and 3 (33); VP, LiP1, and LiP2 from *Ceriporiopsis subvermispora* (44); and VPs from *P. eryngii* (45). The low-redox-potential substrate ABTS is also oxidized with high efficiency by *Tv*DyP1 and in general by DyPs and to a lesser extent by *Tv*VP2; however, Mn^{2+} was only oxidized by *Tv*VP2 at a very low efficiency compared to that of previously characterized VPs (17, 28, 33, 43). Mn^{2+} is generally not oxidized by DyPs, although it has been reported that two DyPs from *P. ostreatus* exhibited Mn^{2+}-oxidizing activity, which was especially significant for *Po*DyP4 (near 200 s^{-1} mM^{-1}) (28). The catalytic efficiency of *Tv*VP2 for Mn^{2+} oxidation was dramatically lower than that of fungal lignin-modifying peroxidases, including VPs and MnPs from *P. ostreatus* (28, 44) and VPs from *C. subvermispora* (44) and *P. eryngii* (45). The high-redox-potential dye RB5, which is a typical VP substrate, was found to be not or poorly oxidized by *Tv*DyP1 and DyPs from other fungi, with the exception of the two DyPs from *A. auricula-judae* and *P. ostreatus* (26, 28, 29). Unlike *Tv*DyP1 but similar to what has been previously reported for VPs from *P. ostreatus* (33) and *P. eryngii* (45), RB5 was very efficiently oxidized by *Tv*VP2 (k_{cat}/K_m, 2,640 s^{-1} mM^{-1}). In fact, *Tv*VP2 presented the greatest apparent affinity for both high-redox-potential dye substrates RB5 and RB19 (K_m, 10.2 and 31.2 μM, respectively). *Tv*DyP1 was also able to oxidize RB19 (K_m, 37.8 μM), a typical DyP substrate, very similarly to *Tv*VP2 (K_m, 31.2 μM). Both enzymes presented similar catalytic efficiencies (k_{cat}/K_m, 629.6 and 615.4 s^{-1} mM^{-1}) on this substrate that are slightly higher than those previously reported for *P. ostreatus* peroxidases *Po*DyP1 and *Po*VP2 (k_{cat}/K_m, 113 and 495 s^{-1} mM^{-1}, respectively [28]) but 3- to 10-fold lower than those obtained with *P. ostreatus* peroxidases *Po*DyP4 and *Po*VP1 (k_{cat}/K_m, 1,860 and 3,220 s^{-1} mM^{-1}, respectively [28]) and wild type and *E. coli*-expressed *A. auricula-judae* DyP (k_{cat}/K_m, 3,600 and 2,400 s^{-1} mM^{-1}, respectively [29]).

Regarding DMP oxidation, *Tv*DyP1 was 16-fold more efficient than *Tv*VP2 because of its 2.5-fold lower K_m and 6-fold higher k_{cat}. However, both peroxidases presented lower activity on this phenolic substrate than other well-characterized peroxidases, including LiPs and MnPs (28, 44). Oxidation of this particular substrate by *A. auricula-judae* DyP (29) and *Po*VPs (33) previously showed biphasic (sigmoidal) kinetics, enabling the calculation of two sets of kinetic constants. This behavior, as well as other substrate specificities, was explained by computational spectroscopic and site-directed mutagenesis studies of *A. auricula-judae* DyP that revealed the existence of more than one oxidation site with different turnover values and substrate affinities (30). In the present study, similar patterns were not obtained with any substrate tested with both enzymes.

During wood degradation, *T. versicolor* has to cope with many compounds, including terpenes and flavonoids. We observed that both of the peroxidases investigated in this study can oxidize flavonoids such as CAT and QUE, compounds known to be oxidized by various oxidases and peroxidases (36, 46–48). Under the conditions used in our experiments, *Tv*VP2 was more active than *Tv*DyP1 on both of these flavonoids. Both peroxidases induced a large modification of the CAT absorbance spectrum, in particular an increase in absorbance at 400 nm. This spectrum modification could correspond to the formation of two quinone groups on the B ring (46). In addition, this oxidation could lead to polymers that are not detectable by high-performance liquid chromatography (HPLC). Concerning QUE, *Tv*VP2 induced both the appearance of an absorbance peak at 290 nm and a decrease in absorbance at 370 nm. In contrast the increase in absorbance at 290 nm was not detected in the case of oxidation by *Tv*DyP1,

suggesting another mechanism of oxidation. For instance, QUE has been shown to be a substrate of several peroxidases/oxidases, with the formation of quinones on different sites (47, 48).

Considering potential applications for these two peroxidases, the ability to decolorize representatives of the main dye families used in industry was tested, revealing that, globally, *Tv*VP2 presented a wider range of action than *Tv*DyP1 and potential for this application. The two *T. versicolor* enzymes showed diverse properties, confirming the contribution of biodiversity screening to the discovery of new biocatalysts. To go further in this research, future directed-mutagenesis experiments and crystallographic studies using the *Tv*DyP1 and *Tv*VP2 heterologous expression system developed here will be set up to explain enzyme substrate specificities and develop more robust enzymes for biotechnological applications.

MATERIALS AND METHODS

Materials. DTT, lysozyme, glutathione, hemin, DMP, VA, RB19, CAT hydrate (98% pure; molecular weight [MW], 290.27), QUE (95% pure; MW, 302.24), hydrogen peroxide solution (50% [wt/wt] in water, stabilized), reduced L-glutathione (98% pure; MW, 307.32), and dibasic sodium phosphate (99% pure; BioReagents) were purchased from Sigma-Aldrich (Steinheim, Germany); isopropyl-β-D-thiogalactopyranoside (IPTG) was from Calbiochem (Meudon, France); ABTS was from Boehringer Mannheim (Saint-Quentin Fallavier, France); and sodium phosphate monobasic dehydrate was obtained from Euromedex (Souffelweyersheim, France). The industrial dyes AB, RB5, Disperse Blue 79 (DB), BB, and Vat Green 1 (VG) were supplied by the SETAS Company (Tekirdağ, Turkey).

Strain and growth medium. The dikaryon *T. versicolor* was deposited in the CIRM-CF collection under no. BRFM 1218. *T. versicolor* BRFM 1218 was collected on oak (*Quercus pubescens*) in Goult (Vaucluse, France). To confirm the morphological identification, molecular identification by internal transcribed spacer (ITS; ITS1, ITS2, and 5.8S rRNA) sequencing was performed. The sequence was compared by similarity analysis (BLASTn) to those in GenBank and FunGene-DB (49), and it corresponded unequivocally to the species *T. versicolor*. The fungus was grown on 4% malt extract agar medium, and three oak sapwood wood blocks (25 by 15 by 5 mm) were then placed on the grown mycelium after 2 weeks of incubation. The blocks were dried for 48 h at 103°C before use. Incubation was carried out at 25°C in the dark. Oak blocks colonized for 1 month were removed carefully from the agar plates, and the mycelium surrounding the blocks was excised. The secretome was extracted by soaking the wood chips in potassium acetate buffer (100 mM, pH 4.5) for 120 min at room temperature. The secretome obtained was stored at −20°C before further analysis. The total amount of proteins was assessed with the Bradford assay (Protein Assay Dye Reagent Concentrate; Bio-Rad, Ivry, France) with bovine serum albumin standard concentrations that ranged from 0.2 to 1 mg · ml^{-1}.

Proteomic analysis of the secretome. Short SDS-PAGE runs (precast 4 to 12% Bis-Tris minigels; Invitrogen, France) were performed, allowing proteins diafiltered from the secretome (15 μg) to migrate on a 0.5-cm length, and gels were stained with Coomassie blue (Bio-Rad, Marnes-la-Coquette, France). Each gel electrophoresis lane was cut into two slices (2 mm wide), and protein identification was performed by the PAPPSO (Plate-forme d'Analyze Protéomique de Paris Sud-Ouest) platform facilities. In-gel digestion was carried out in accordance with a standard trypsinolysis protocol. Gel pieces were washed twice with 50% (vol/vol) acetonitrile (ACN)–25 mM NH_4CO_3 and incubated in the presence of 10 mM DTT for 1 h at 56°C. After cooling, the supernatant was removed and the samples were incubated with 55 mM iodoacetamide at room temperature in the dark. Gel plugs were washed with ACN and then dried in a vacuum concentrator (Thermo Fisher Scientific, Villebon sur Yvette, France). Digestion was performed for 8 h at 37°C with 200 ng of modified trypsin (Promega, Charbonnières-les-Bains, France) dissolved in 25 mM NH_4CO_3. Tryptic peptides were extracted first with 50% (vol/vol) ACN–0.5% (vol/vol) trifluoroacetic acid (TFA) and then with pure ACN. Peptide extracts were dried in a vacuum speed concentrator (Thermo Fisher Scientific, Villebon sur Yvette, France) and suspended in 25 μl of 2% (vol/vol) ACN–0.05% (vol/vol) TFA–0.08% (vol/vol) formic acid. HPLC was performed on a NanoLC-Ultra system (Eksigent, Les Ulis, France). Tryptic digestion products were first concentrated and desalted on a precolumn cartridge (PepMap 100 C_{18}, 0.3 by 5 mm, Dionex; Thermo Fisher Scientific) with 0.1% formic acid at 7.5 μl min^{-1} for 3 min. The precolumn cartridge was connected to the separating column (C_{18}, 0.075 by 15 cm; Biosphere Nanoseparations, Nieuwkoop, The Netherlands), and the peptides were eluted with a linear gradient of 5 to 35% ACN in 0.1% formic acid for 40 min at 300 nl · min^{-1}. On-line analysis of peptides was performed with a Q-exactive mass spectrometer (Thermo Fisher Scientific, United States) with a nanoelectrospray ion source. Ionization (1.8-kV ionization potential) was performed with a stainless steel emitter (30-μm inner diameter; Thermo Electron, Villebon sur Yvette, France). Peptide ions were analyzed with Xcalibur 2.1 software (Thermo Scientific, Villebon sur Yvette, France) with the following data-dependent acquisition steps: step 1, full MS scan (mass-to-charge ratio [*m/z*] 400 to 1,400; resolution, 70,000); step 2, tandem MS (MS/MS; normalized collision energy, 30%; resolution, 17,500). Step 2 was repeated for the eight major ions detected in step 1. Dynamic exclusion was set to 40 s. The raw mass data were first converted to mzXML format with the ReAdW software (SPC Proteomics Tools, Seattle, WA). Protein identification was performed by querying the MS/MS data against databases, together with an in-house contaminant database, with the X!Tandem software (X!Tandem Cyclone, Jouy en Josas, France) and the following parameters: one trypsin missed, cleavage allowed, alkylation of

cysteine, conditional oxidation of methionine, and precursor and fragment ion set at 2 ppm and 0.005 Da, respectively. A refined search with similar parameters was added, except that semitryptic peptides, possible N-term acetylation, and histidine mono- and dimethylations were also searched. All peptides matched with an E value of <0.05 were parsed with X!Tandem pipeline software. Proteins identified with at least two unique peptides and a log E value of <-2.6 were validated.

Gene synthesis. The mature protein-coding sequences of a DyP and a VP (GenBank accession numbers 19415892 and 19412643) encoding the proteins with Joint Genome Institute (JGI) protein ID no. 48870 and 26239 from *T. versicolor* (FP-101664 SS1, corresponding to *Tv*DyP1 and *Tv*VP2, respectively) were synthesized by GeneArt Gene Synthesis (Life Technologies, Germany) after codon optimization for *E. coli* expression.

***Tv*DyP1 production in *E. coli*.** The *Tv*DyP1 coding sequence was cloned into the pET23b(+) vector (Novagen, Darmstadt, Germany), and the resulting plasmid (pET23b-*Tv*DyP1) was used for expression in *E. coli* BL21(DE3) (Invitrogen, GeneArt, Regensburg, Germany). Cells were grown for 3 h at 37°C in terrific broth (TB) containing 100 μg · ml^{-1} ampicillin, induced with 1 mM IPTG, and grown further for 48 h at 16°C in the presence of 20 μM hemin. Cells were harvested by centrifugation at 8,000 rpm for 10 min at 4°C. The bacterial pellet was resuspended in 100 ml of lysis buffer (20 mM Tris-HCl [pH 8.0] containing 1 mM EDTA and 5 mM DTT) supplemented with lysozyme (Sigma-Aldrich) at 2 mg · ml^{-1}, DNase I, and a protease inhibitor cocktail (Roche Diagnostics, Mannheim, Germany). After 1 h of incubation, cells were sonicated and then centrifuged at 12,000 rpm for 30 min to remove cell debris. The resulting supernatant was dialyzed first against 20 mM acetate, pH 4.3, and then further dialyzed against 20 mM Tris, pH 7.5. Insoluble material was removed after each dialysis step (12,000 rpm for 10 min). *Tv*DyP1 was purified with an ÄKTA Express purification system (GE Healthcare Bio-Sciences AB, Uppsala, Sweden) in two consecutive steps. First, the *Tv*DyP1 solution was loaded onto a 1-ml Mono Q 5/50 GL column (GE Healthcare Bio-Sciences AB, Uppsala, Sweden) in 20 mM Tris (pH 7.5) buffer at a flow rate of 1 ml · min^{-1}. After column washing with the buffer described above, two successive linear NaCl concentration gradients (0 to 0.15 and 0.15 to 0.5 M NaCl) were applied for 20 and 10 min, respectively.

Peroxidase activity was monitored by measuring ABTS oxidation in the presence of H_2O_2 as described below. The active fractions were pooled, dialyzed against 20 mM Tris (pH 7.5), and loaded into a 20-ml Q-Sepharose column (GE Healthcare Bio-Sciences AB) in the same buffer at a flow rate of 1 ml · min^{-1}. Proteins were then eluted with a 0 to 0.5 M NaCl gradient for 20 min. *Tv*DyP1 purification was checked by SDS-PAGE in a 12% gel stained with Coomassie brilliant blue R-250 (Sigma). The electronic absorption spectrum of the purified enzyme was recorded with an Agilent 8453 diode array UV-visible spectrophotometer (Agilent Technologies, Santa Clara, CA).

***Tv*VP2 production in *E. coli*.** The *Tv*VP2 coding sequence was cloned into the pET23b(+) vector (Novagen), and the resulting plasmid (pET23b-*Tv*VP2) was used for expression in *E. coli* BL21(DE3) (Invitrogen). Cells were grown for 3 h at 37°C in TB containing 100 μg · ml^{-1} ampicillin, induced with 1 mM IPTG, and grown for 4 h. *Tv*VP2 accumulated in inclusion bodies, as observed by SDS-PAGE, and was solubilized with 8 M urea. *In vitro* refolding was performed in 0.16 M urea–5 mM Ca^{2+}–20 μM hemin–0.5 mM oxidized glutathione–0.1 mM dithiothreitol–0.1 mg · ml^{-1} protein at pH 9.5 as previously described (28).

*Tv*VP2 was purified by a one-step chromatographic procedure with an ÄKTA Express purification system (GE Healthcare Bio-Sciences AB, Uppsala, Sweden) and a Mono Q 5/50 GL column (GE Healthcare Bio-Sciences AB) with a 0 to 0.5 M NaCl gradient (1 ml · min^{-1}, 40 min) in 10 mM tartrate (pH 5.5) containing 1 mM $CaCl_2$.

N-terminal sequencing and MS. To determine the N-terminal sequence of the purified peroxidases and those of the fragments generated by partial proteolysis, the protein material was subjected to protein sequence analysis on an Applied Biosystems 476A sequencer by the proteomic platform of the Institut de Microbiologie de la Méditerrranée, CNRS, Aix-Marseille Université. Matrix-assisted laser desorption ionization–time of flight MS of samples was carried out on a Microflex II time of flight mass spectrometer (Bruker Daltonik, Germany).

Optimum pH determination. The optimal pH for substrate oxidation by each of the two *T. versicolor* peroxidases was determined by measuring the enzymatic activity with saturating concentrations of RB5 (30 μM), RB19 (200 μM), ABTS (5 mM), DMP (20 and 60 mM for *Tv*VP2 and *Tv*DyP1, respectively), VA (20 mM), and Mn^{2+} (10 mM) in 0.1 M tartrate buffer as described below.

Peroxidase kinetic studies. The kinetic constants of *T. versicolor* *Tv*DyP1 and *Tv*VP2 were estimated from the absorbance changes observed during substrate oxidation at the optimal pH at 30°C in a Uvikon XS spectrophotometer (BioTek Instruments, Colmar, France) (29). Depending on the substrate, different concentrations of H_2O_2 were added to initiate the reaction. Oxidation of ABTS was determined by measuring the generation of its cation radical (ε_{436} = 29,300 M^{-1} cm^{-1}). RB5 and RB19 oxidation was monitored for colorant disappearance (ε_{598} = 30 mM^{-1} cm^{-1} and ε_{595} = 10 mM^{-1} cm^{-1}, respectively). Oxidation of Mn^{2+} was determined by monitoring Mn^{3+}-tartrate complex (ε_{238} = 6.5 mM^{-1} cm^{-1}) formation. VA oxidation was determined for veratraldehyde (ε_{310} = 9.3 mM^{-1} cm^{-1}) formation. DMP oxidation was monitored for dimeric coerulignone (ε_{469} = 55 mM^{-1} cm^{-1}). All enzymatic activities were measured as initial velocities taking linear increments (decreases for RB5 and RB19). Mean apparent affinity constant (Michaelis constant, K_m) and enzyme turnover (catalytic constant, k_{cat}) values and standard errors were obtained by nonlinear least-squares fitting to the Michaelis-Menten model. Fitting of these constants to the normalized Michaelis-Menten equation $v = (k_{cat}/K_m)[S]/(1+[S]/K_m)$ yielded enzyme efficiency values (k_{cat}/K_m) with their standard errors.

pH stability studies. To study the effect of pH on *T. versicolor* peroxidase stability, the enzymes were incubated in 0.1 M tartrate buffer at pH 2 to 6 and kept at room temperature for different time periods.

Residual activities were measured after 1 min of incubation (to evaluate the initial survival of the enzyme at each pH) and 30, 60, 120, and 180 min of incubation for *Tv*VP2 and 24 and 48 h for *Tv*DyP1. The activity obtained with the sample incubated for 1 min at pH 5 was taken as a reference (maximum activity). Activity was determined by oxidation of a saturating concentration of ABTS in 0.1 M tartrate at the optimal pH of each enzyme (3.0 for *Tv*VP2 and 3.5 for *Tv*DyP1) under the conditions described above.

Thermal stability studies. To study the thermal stability of *T. versicolor* peroxidases, the enzymes were incubated in 0.1 M tartrate buffer (pH 5.0) over a range of 25 to 70°C. Residual activity was determined after 1, 30, 60, 120, and 180 min after a cooling step on ice. The activity of the enzyme incubated at 4°C was taken as a reference (maximum activity) to calculate the percentage of residual activity at any time.

Effect of hydrogen peroxide. The effects of different H_2O_2 concentrations on peroxidase activity were determined under standard assay conditions at the optimal pH for each enzyme (3.0 for *Tv*VP2 and 3.5 for *Tv*DyP1).

Natural plant molecule (CAT and QUE) oxidation by peroxidases. Oxidation of CAT hydrate and QUE was determined at room temperature by analyzing the spectra of both flavonoids between 250 and 600 nm. Additional kinetic experiments were conducted by determining the absorbance at 400 and 370 nm, corresponding to the characteristic peaks of CAT hydrate and QUE, respectively. These experiments were carried out with a Cary 50 spectrophotometer (Agilent Technologies). CAT and QUE were used at 20 and 10 μM, respectively. For both compounds, reactions were carried out in 100 mM phosphate buffer (pH 5.8). For some conditions, CAT and QUE were incubated in the presence of 1 mM H_2O_2. For these assays, the concentration of the peroxidases tested was 0.2 μM.

Industrial dye decolorization by peroxidases. To test the abilities of peroxidases to decolorize industrial dyes, five dyes, AB, RB5, DB, BB, and VG, were selected. Dyes were kindly provided by the SETAS Company (Çerkezköy, Turkey). They were prepared from either powder dyes, i.e., AB (0.005% [vol/vol]), RB (0.005% [vol/vol]), and DB (0.01% [vol/vol]), prepared in 0.1 M sodium tartrate buffer (pHs 2.5, 3.0, and 3.5), or liquid dyes, i.e., BB (0.002% [vol/vol]) and VG (0.01% [vol/vol]), in each buffer (pHs 2.5, 3.0, and 3.5). Enzymatic dye decolorization capacity was assayed in 96-well microplates by adding 2 μl of H_2O_2 and 0.4 μg of enzyme to 200 μl of dye solution in sodium tartrate buffer at pHs 2.5, 3, and 3.5. Two controls were performed under the same conditions without H_2O_2 or without enzyme. The decolorization of AB, RB5, DB, BB, and VG was measured at 37°C at wavelengths of 560, 610, 530, 610, and 640 nm, respectively. Percent decolorization was calculated with the following formula: % decolorization = [(Abs t_0 − Abs t)/Abs t_0] × 100, where Abs t_0 is the optical density at the beginning of the experiment (t_0) and Abs t is the optical density after 1 h of incubation, as indicated in the legend of Table 4.

Accession number(s). The ITS sequence obtained in this study was deposited in GenBank under accession number MG554226.

SUPPLEMENTAL MATERIAL

Supplemental material for this article may be found at https://doi.org/10.1128/AEM.02826-17.

SUPPLEMENTAL FILE 1, PDF file, 0.4 MB.

ACKNOWLEDGMENTS

We are grateful to the European Commission for funding this work within the INDOX project (KBBE-2013-7-613549). This study was also funded by a grant from the French National Research Agency (ANR) as part of the Investissements d'Avenir program (ANR-11-LABX-0002-01, Lab of Excellence ARBRE).

We thank the SETAS Company for kindly providing the industrial dyes and Régine Lebrun and Pascal Mansuelle of the proteomics platform of the Institut de Microbiologie de la Méditerranée, CNRS-AMU, Marseille, France, for protein identification by MS. We thank Bernard Rivoire for collecting, identifying, and isolating *T. versicolor* BRFM 1218.

REFERENCES

1. Gao D, Du L, Yang J, Wu WM, Liang H. 2010. A critical review of the application of white rot fungus to environmental pollution control. Crit Rev Biotechnol 30:70–77. https://doi.org/10.3109/07388550903427272.
2. Nagy LG, Riley R, Bergmann PJ, Krizsan K, Martin FM, Grigoriev IV, Cullen D, Hibbett DS. 2017. Genetic bases of fungal white rot wood decay predicted by phylogenomic analysis of correlated gene-phenotype evolution. Mol Biol Evol 34:35–44. https://doi.org/10.1093/molbev/msw238.
3. Floudas D, Binder M, Riley R, Barry K, Blanchette RA, Henrissat B, Martínez AT, Otillar R, Spatafora JW, Yadav JS, Aerts A, Benoit I, Boyd A, Carlson A, Copeland A, Coutinho PM, de Vries RP, Ferreira P, Findley K, Foster B, Gaskell J, Glotzer D, Gorecki P, Heitman J, Hesse C, Hori C, Igarashi K, Jurgens JA, Kallen N, Kersten P, Kohler A, Kues U, Kumar TK, Kuo A, LaButti K, Larrondo LF, Lindquist E, Ling A, Lombard V, Lucas S, Lundell T, Martin R, McLaughlin DJ, Morgenstern I, Morin E, Murat C, Nagy LG, Nolan M, Ohm RA, Patyshakuliyeva A, Rokas A, Ruiz-Dueñas FJ, Sabat G, Salamov A, Samejima M, Schmutz J, Slot JC, St John F, Stenlid J, Sun H, Sun S, Syed K, Tsang A, Wiebenga A, Young D, Pisabarro A, Eastwood DC, Martin F, Cullen D, Grigoriev IV, Hibbett DS. 2012. The Paleozoic origin of enzymatic lignin decomposition reconstructed from 31 fungal genomes. Science 336:1715–1719. https://doi.org/10.1126/science.1221748.
4. Grey R, Hofer C, Schlosser D. 1998. Degradation of 2-chlorophenol and formation of 2-chloro-1,4-benzoquinone by mycelia and cell-free crude

culture liquids of *Trametes versicolor* in relation to extracellular laccase activity. J Basic Microbiol 38:371–382. https://doi.org/10.1002/(SICI)1521-4028(199811)38:5/6<371::AID-JOBM371>3.0.CO;2-V.
5. Yemendzhiev H, Gerginova M, Krastanov A, Stoilova I, Alexieva Z. 2008. Growth of *Trametes versicolor* on phenol. J Ind Microbiol Biotechnol 35:1309–1312. https://doi.org/10.1007/s10295-008-0412-z.
6. Asgher M, Bhatti HN, Ashraf M, Legge RL. 2008. Recent developments in biodegradation of industrial pollutants by white rot fungi and their enzyme system. Biodegradation 19:771–783. https://doi.org/10.1007/s10532-008-9185-3.
7. Carabajal M, Ullrich R, Levin L, Kluge M, Hofrichter M. 2012. Degradation of phenol and *p*-nitrophenol by the white-rot polypore *Trametes versicolor*, p 69–72. 5th International Symposium on Biosorption and Bioremediation, 24 to 28 June 2012, Prague, Czech Republic.
8. Chakroun H, Bouaziz M, Dhouib A, Sayadi S. 2012. Enzymatic oxidative transformation of phenols by *Trametes trogii* laccases. Environ Technol 33:1977–1985. https://doi.org/10.1080/09593330.2012.655317.
9. Ruiz-Dueñas FJ, Lundell T, Floudas D, Nagy LG, Barrasa JM, Hibbett DS, Martínez AT. 2013. Lignin-degrading peroxidases in Polyporales: an evolutionary survey based on 10 sequenced genomes. Mycologia 105:1428–1444. https://doi.org/10.3852/13-059.
10. Jönsson LJ, Saloheimo M, Penttila M. 1997. Laccase from the white-rot fungus *Trametes versicolor*: cDNA cloning of lcc1 and expression in *Pichia pastoris*. Curr Genet 32:425–430. https://doi.org/10.1007/s002940050298.
11. Johansson T, Nyman PO. 1993. Isozymes of lignin peroxidase and manganese(II) peroxidase from the white-rot basidiomycete *Trametes versicolor*. I. Isolation of enzyme forms and characterization of physical and catalytic properties. Arch Biochem Biophys 300:49–56.
12. Johansson T, Welinder KG, Nyman PO. 1993. Isozymes of lignin peroxidase and manganese(II) peroxidase from the white-rot basidiomycete *Trametes versicolor*. II. Partial sequences, peptide maps, and amino acid and carbohydrate compositions. Arch Biochem Biophys 300:57–62.
13. Camarero S, Sarkar S, Ruiz-Dueñas FJ, Martínez MJ, Martínez AT. 1999. Description of a versatile peroxidase involved in the natural degradation of lignin that has both manganese peroxidase and lignin peroxidase substrate interaction sites. J Biol Chem 274:10324–10330. https://doi.org/10.1074/jbc.274.15.10324.
14. Ruiz-Dueñas FJ, Camarero S, Perez-Boada M, Martínez MJ, Martínez AT. 2001. A new versatile peroxidase from *Pleurotus*. Biochem Soc Trans 29:116–122. https://doi.org/10.1042/bst0290116.
15. Ruiz-Dueñas FJ, Morales M, Garcia E, Miki Y, Martínez MJ, Martínez AT. 2009. Substrate oxidation sites in versatile peroxidase and other basidiomycete peroxidases. J Exp Bot 60:441–452. https://doi.org/10.1093/jxb/ern261.
16. Martínez MJ, Ruiz-Dueñas FJ, Guillen F, Martínez AT. 1996. Purification and catalytic properties of two manganese peroxidase isoenzymes from *Pleurotus eryngii*. Eur J Biochem 237:424–432. https://doi.org/10.1111/j.1432-1033.1996.0424k.x.
17. Heinfling A, Ruiz-Dueñas FJ, Martínez MJ, Bergbauer M, Szewzyk U, Martínez AT. 1998. A study on reducing substrates of manganese-oxidizing peroxidases from *Pleurotus eryngii* and *Bjerkandera adusta*. FEBS Lett 428:141–146. https://doi.org/10.1016/S0014-5793(98)00512-2.
18. Carabajal M, Kellner H, Levin L, Jehmlich N, Hofrichter M, Ullrich R. 2013. The secretome of *Trametes versicolor* grown on tomato juice medium and purification of the secreted oxidoreductases including a versatile peroxidase. J Biotechnol 168:15–23. https://doi.org/10.1016/j.jbiotec.2013.08.007.
19. Welinder KG, Mauro JM, Norskov-Lauritsen L. 1992. Structure of plant and fungal peroxidases. Biochem Soc Trans 20:337–340. https://doi.org/10.1042/bst0200337.
20. Hofrichter M, Ullrich R, Pecyna MJ, Liers C, Lundell T. 2010. New and classic families of secreted fungal heme peroxidases. Appl Microbiol Biotechnol 87:871–897. https://doi.org/10.1007/s00253-010-2633-0.
21. Sugano Y. 2009. DyP-type peroxidases comprise a novel heme peroxidase family. Cell Mol Life Sci 66:1387–1403. https://doi.org/10.1007/s00018-008-8651-8.
22. Kim SJ, Ishikawa K, Hirai M, Shoda M. 1995. Characteristics of a newly isolated fungus, *Geotrichum candidum* Dec 1, which decolorizes various dyes. J Ferment Bioeng 79:601–607. https://doi.org/10.1016/0922-338X(95)94755-G.
23. Johjima T, Ohkuma M, Kudo T. 2003. Isolation and cDNA cloning of novel hydrogen peroxide-dependent phenol oxidase from the basidiomycete *Termitomyces albuminosus*. Appl Microbiol Biotechnol 61:220–225. https://doi.org/10.1007/s00253-003-1236-4.
24. Pühse M, Szweda RT, Ma Y, Jeworrek C, Winter R, Zorn H. 2009. *Marasmius scorodonius* extracellular dimeric peroxidase—exploring its temperature and pressure stability. Biochim Biophys Acta 1794:1091–1098. https://doi.org/10.1016/j.bbapap.2009.03.015.
25. Liers C, Bobeth C, Pecyna M, Ullrich R, Hofrichter M. 2010. DyP-like peroxidases of the jelly fungus *Auricularia auricula-judae* oxidize nonphenolic lignin model compounds and high-redox potential dyes. Appl Microbiol Biotechnol 85:1869–1879. https://doi.org/10.1007/s00253-009-2173-7.
26. Salvachúa D, Prieto A, Martínez AT, Martínez MJ. 2013. Characterization of a novel dye-decolorizing peroxidase (DyP)-type enzyme from *Irpex lacteus* and its application in enzymatic hydrolysis of wheat straw. Appl Environ Microbiol 79:4316–4324. https://doi.org/10.1128/AEM.00699-13.
27. Liers C, Pecyna MJ, Kellner H, Worrich A, Zorn H, Steffen KT, Hofrichter M, Ullrich R. 2013. Substrate oxidation by dye-decolorizing peroxidases (DyPs) from wood- and litter-degrading agaricomycetes compared to other fungal and plant heme-peroxidases. Appl Microbiol Biotechnol 97:5839–5849. https://doi.org/10.1007/s00253-012-4521-2.
28. Fernández-Fueyo E, Linde D, Almendral D, Lopez-Lucendo MF, Ruiz-Dueñas FJ, Martínez AT. 2015. Description of the first fungal dye-decolorizing peroxidase oxidizing manganese(II). Appl Microbiol Biotechnol 99:8927–8942. https://doi.org/10.1007/s00253-015-6665-3.
29. Linde D, Coscolin C, Liers C, Hofrichter M, Martínez AT, Ruiz-Dueñas FJ. 2014. Heterologous expression and physicochemical characterization of a fungal dye-decolorizing peroxidase from *Auricularia auricula-judae*. Protein Expr Purif 103:28–37. https://doi.org/10.1016/j.pep.2014.08.007.
30. Linde D, Pogni R, Canellas M, Lucas F, Guallar V, Baratto MC, Sinicropi A, Sáez-Jiménez V, Coscolin C, Romero A, Medrano FJ, Ruiz-Dueñas FJ, Martínez AT. 2015. Catalytic surface radical in dye-decolorizing peroxidase: a computational, spectroscopic and site-directed mutagenesis study. Biochem J 466:253–262. https://doi.org/10.1042/BJ20141211.
31. Roberts JN, Singh R, Grigg JC, Murphy ME, Bugg TD, Eltis LD. 2011. Characterization of dye-decolorizing peroxidases from *Rhodococcus jostii* RHA1. Biochemistry 50:5108–5119. https://doi.org/10.1021/bi200427h.
32. Strittmatter E, Liers C, Ullrich R, Wachter S, Hofrichter M, Plattner DA, Piontek K. 2013. First crystal structure of a fungal high-redox potential dye-decolorizing peroxidase: substrate interaction sites and long-range electron transfer. J Biol Chem 288:4095–4102. https://doi.org/10.1074/jbc.M112.400176.
33. Fernández-Fueyo E, Ruiz-Dueñas FJ, Martínez MJ, Romero A, Hammel KE, Medrano FJ, Martínez AT. 2014. Ligninolytic peroxidase genes in the oyster mushroom genome: heterologous expression, molecular structure, catalytic and stability properties, and lignin-degrading ability. Biotechnol Biofuels 7:2. https://doi.org/10.1186/1754-6834-7-2.
34. Valderrama B, Ayala M, Vazquez-Duhalt R. 2002. Suicide inactivation of peroxidases and the challenge of engineering more robust enzymes. Chem Biol 9:555–565. https://doi.org/10.1016/S1074-5521(02)00149-7.
35. Zhang B, Cai J, Duan CQ, Reeves MJ, He F. 2015. A review of polyphenolics in oak woods. Int J Mol Sci 16:6978–7014. https://doi.org/10.3390/ijms16046978.
36. Oszmianski J, Lee CY. 1990. Enzymic oxidative reaction of catechin and chlorogenic acid in a model system. J Agric Food Chem 38:1202–1204. https://doi.org/10.1021/jf00095a009.
37. Sokolová R, Ramešová Š, Degano I, Hromadová M, Gál M, Žabka J. 2012. The oxidation of natural flavonoid quercetin. Chem Commun (Camb) 48:3433–3435. https://doi.org/10.1039/c2cc18018a.
38. Gomi N, Yoshida S, Matsumoto K, Okudomi M, Konno H, Hisabori T, Sugano Y. 2011. Degradation of the synthetic dye amaranth by the fungus *Bjerkandera adusta* Dec 1: inference of the degradation pathway from an analysis of decolorized products. Biodegradation 22:1239–1245. https://doi.org/10.1007/s10532-011-9478-9.
39. Sugano Y, Matsuo C, Shoda M. 2001. Efficient production of a heterologous peroxidase, DyP from *Geotrichum candidum* Dec 1, on solid-state culture of *Aspergillus oryzae* RD005. J Biosci Bioeng 92:594–597. https://doi.org/10.1016/S1389-1723(01)80323-6.
40. Sugano Y, Ishii Y, Shoda M. 2004. Role of H164 in a unique dye-decolorizing heme peroxidase DyP. Biochem Biophys Res Commun 322:126–132. https://doi.org/10.1016/j.bbrc.2004.07.090.
41. Shimokawa T, Shoda M, Sugano Y. 2009. Purification and characterization of two DyP isozymes from *Thanatephorus cucumeris* Dec 1 specifically expressed in an air-membrane surface bioreactor. J Biosci Bioeng 107:113–115. https://doi.org/10.1016/j.jbiosc.2008.09.013.
42. Pérez-Boada M, Doyle WA, Ruiz-Dueñas FJ, Martînez MJ, Martînez AT, Smith AT. 2002. Expression of *Pleurotus eryngii* versatile peroxidase in

Escherichia coli and optimisation of *in vitro* folding. Enzyme Microb Technol 30:518–524. https://doi.org/10.1016/S0141-0229(02)00008-X.
43. Sáez-Jiménez V, Fernández-Fueyo E, Medrano FJ, Romero A, Martínez AT, Ruiz-Dueñas FJ. 2015. Improving the pH-stability of versatile peroxidase by comparative structural analysis with a naturally-stable manganese peroxidase. PLoS One 10:e0140984. https://doi.org/10.1371/journal.pone.0140984.
44. Fernández-Fueyo E, Ruiz-Dueñas FJ, Miki Y, Martínez MJ, Hammel KE, Martínez AT. 2012. Lignin-degrading peroxidases from genome of selective ligninolytic fungus *Ceriporiopsis subvermispora*. J Biol Chem 287:16903–16916. https://doi.org/10.1074/jbc.M112.356378.
45. Bao X, Liu A, Lu X, Li JJ. 2012. Direct over-expression, characterization and H_2O_2 stability study of active *Pleurotus eryngii* versatile peroxidase in *Escherichia coli*. Biotechnol Lett 34:1537–1543. https://doi.org/10.1007/s10529-012-0940-5.
46. Moridani MY, Scobie H, Salehi P, O'Brien PJ. 2001. Catechin metabolism: glutathione conjugate formation catalyzed by tyrosinase, peroxidase, and cytochrome p450. Chem Res Toxicol 14:841–848. https://doi.org/10.1021/tx000235o.
47. Kubo I, Nihei K, Shimizu K. 2004. Oxidation products of quercetin catalyzed by mushroom tyrosinase. Bioorg Med Chem 12:5343–5347. https://doi.org/10.1016/j.bmc.2004.07.050.
48. Awad HM, Boersma MG, Vervoort J, Rietjens IM. 2000. Peroxidase-catalyzed formation of quercetin quinone methide-glutathione adducts. Arch Biochem Biophys 378:224–233. https://doi.org/10.1006/abbi.2000.1832.
49. Navarro D, Favel A, Chabrol O, Pontarotti P, Haon M, Lesage-Meessen L. 2012. FunGene-DB: a web-based tool for Polyporales strains authentication. J Biotechnol 161:383–386. https://doi.org/10.1016/j.jbiotec.2012.06.023.